



POSTER |

VÝZNAM POSTERU

jde o plakát, který zveřejňuje výsledky práce veřejnosti (konference, veřejné prostory, ...)

Může jít i o poutač, reklamní sdělení

Účelem je

- upoutat pozornost
- Představit dosažené výsledky jednoduchou formou / zhodnocení výsledků
- Vyvolat diskuzi při prezentování

OBSAH POSTERU

1. **hlavička (nadpis)** – **místo** konání akce, kde se prezentuje, **název** (čitelný z několika metrů), **autor** (může být s fotografií), **afiliace** (pracoviště)
2. **abstrakt (abstract)** – stručné shrnutí obsahu práce, obvykle i v angličtině, smysl celého příspěvku (shrnutí výsledků), často bývá definován organizátory akce
3. **úvod (introduction)** – fakta týkající se daného tématu, cíle a hypotézy
4. **materiál a metody (methods)** – použitá technika, specifikace vzorku, schémata
5. **výsledky (results)** – uvedení zjištěných výsledků, statistické zpracování, grafy, tabulka
6. **Diskuze (discussion)** – zhodnocení výsledků a komentář k nim
7. **Shrnutí (conclusion)** – stěžejní závěry
8. **literatura (references)** – uvedení citací pokud je nutné (pokud ano, tak ve správné citační normě)
9. **poděkování (acknowledgement)** – podpora projektu, projektové číslo

OBEČNÉ PŘEDPOKLADY

1. čitelnost

- Velikost posteru cca A0 (84,1 x 118,9 cm apod.)
- Název posteru čitelný z 5-10m (velikost fontu cca 70-100 bodů)
- Vlastní obsah čitelný z 1-2m (velikost fontu 16-22 bodů)
- Typ písma – patkové pro běžný psaný text, bezpatkové pro nadpisy

2. přehlednost

- Čím méně textu tím lépe, heslovitě, odrážky
- Text se lépe nahradí obrázky s komentářem
- Nejdůležitější části zvýraznit, orámečkovat, tučné písmo
- Jednotlivé části řadit logicky shora dolů

Developing and characterising a novel combined nanoelectrode system

L. P. Robinson, A. Mount



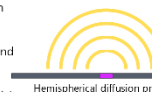
Electrochemistry at nanoelectrodes

Nanoelectrodes have several advantages for electrochemical sensing.



Linear diffusion profile

Transport to macroelectrodes proceeds through a relatively inefficient linear diffusion profile. They are also highly affected by convection or iR drop. They can reliably detect very low (attomole) concentrations of analyte.



Hemispherical diffusion profile

In contrast, the diffusion pattern for nanoelectrodes quickly becomes hemispherical. This profile is much more efficient, and they are not so affected by convection or iR drop. They can reliably detect very low (attomole) concentrations of analyte.

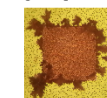
A Pt microsquare nanoband edge electrode (MNEE) array system in which the Pt nanoband acts as the working electrode has been developed. The project now aims to create a nanoelectrode device based on this system which has all three electrodes necessary for analysis on one chip.

Ag/AgCl as a combined electrode

The combined reference/counter electrode is created by electroplating a thin film of Ag onto the Pt microsquare.

Potentiostatic plating causes Ag to grow preferentially at the corners, creating dendrites. A galvanostatic plating protocol is being developed to provide the required smooth, shiny Ag deposit.

To convert the newly plated Ag surface to AgCl, it must be functionalised. Chemical functionalisation by immersion in FeCl₃ has been shown to produce uniform deposits of AgCl.



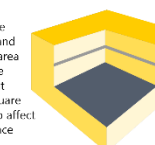
Dendritic growth

Combined nanoelectrode system

This design consists of a microsquare at the bottom of each cavity in the array, with the nanoband around the cavity edge.

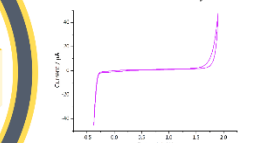
The Ag/AgCl microsquare is a combined reference and counter electrode. As its area is so much larger than the Pt nanoband, the current passing through the square is not large enough to affect its use as the reference electrode.

This could create an on-chip device for sensitive analytical detection.



Characterisation

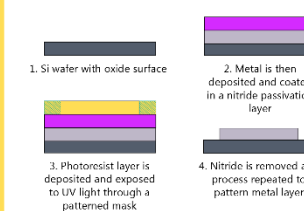
Cyclic voltammetry and electrochemical impedance spectroscopy will be used to verify that the system is behaving as predicted. The nanoband should have a similar response to the current nanoelectrode array.



Example of a nanoelectrode cycling in 100mM KCl solution. This cycle is used to determine the cleanliness of the electrode surface.

Fabrication

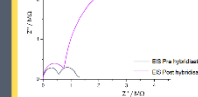
This design has been fabricated at the Scottish Microelectronics Centre using photolithography. In this technique layers of metal and insulator are deposited and patterned to produce the desired arrangement.



Each layer is deposited and patterned sequentially. This approach reliably produces uniform electrodes cheaply and easily.

An application

By coating the surface of the working electrode in a probe nucleic acid, the corresponding DNA sequence can be detected using electrochemical impedance spectroscopy (EIS). Before the target molecule is hybridised, the resistance measured for the redox couple is small. When the correct target is hybridised the resistance, and therefore the EIS response, is much larger.



EIS measurement of 50 nm electrode shows the increase in resistance upon addition of the target nucleic acid.

Pre hybridisation - the redox species has access to the electrode. Post hybridisation - the access of the redox species is restricted, and so the resistance rises at the electrode.

Objectives

Having made the initial measurements, the next steps will include:

- complete fabrication of the combined system, including optimisation of nanoband and cavity dimensions
- further investigation of the sensitivity of nanoelectrodes for use in DNA sensing and the relationship between the response and concentration of the target
- optimisation of a galvanostatic silver plating protocol

Many thanks to Dr Damian Corrigan, Ilka Schmuesser, Professor Andy Mount, the Mount group and the SMC for their continuing support and expertise.



Performance Characterization, Sensitivity and Comparison of a Dual Layer Thermal Protection System



Cole D. Kazemba - Georgia Tech Space Systems Design Laboratory

Advisors: Dr. Robert Braun and Dr. Ian Clark

Co-Authors: Mary Kathy McGuire & Austin Howard - NASA Ames Research Center



Motivation

With the goal of landing high-mass cargo or crewed missions on Mars, NASA has been aiming to develop new thermal protection technologies with enhanced capability and reduced mass compared to traditional approaches.^{1,2} A study was conducted on a dual layer thermal protection system (TPS) to identify sensitivities in performance to uncertainties in material properties and aerothermal environments. A performance metric which is independent of the system construction was developed in order to directly compare the results of the traditional, dual layer and eventually, flexible thermal protection systems.

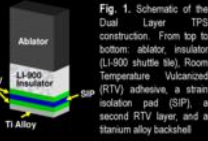


Fig. 1. Schematic of the Dual Layer TPS construction. From top to bottom: Ablator, LI-900 insulator (LI-900 shuttle tile), Room Temperature Vulcanized (RTV) adhesive, a strain isolation pad (SIP), a second RTV layer, and a titanium alloy backshell.

Quantifying Performance

One of the primary goals of this study was to develop a metric to quantify and compare the performance of not just a dual layer or traditional TPS, but any thermal protection system. The purpose of developing such a performance metric is to assess TPS design efficiency while including characteristics of the trajectory rather than simply using the masses of the systems. In order to capture the ability of a thermal protection system in regard to both the trajectories it can fly and the mass required to do so, a new TPS performance metric was established. This metric, Specific Heat Load (Q_{sp}), is a ratio of the total integrated heat load seen by the TPS to the required areal mass to successfully fly that trajectory while protecting the vehicle.

$$Specific\ Heat\ Load, Q_{sp} = \frac{Total\ Integrated\ Heat\ Load}{Total\ TPS\ Areal\ Mass}$$

Trajectory Investigated

The test case used for this study consisted of a mid LD rigid aerobically vehicle on a dual heat pulse trajectory. The first pulse would slow the vehicle from its hyperbolic approach trajectory to a parking orbit via aerobrake within Mars' atmosphere. Following a long on-orbit cool off period, the vehicle would then perform an entry maneuver through the atmosphere and down to the Martian surface.

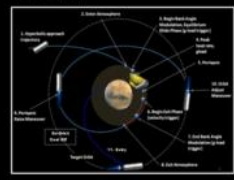


Fig. 2. Events leading from the hyperbolic approach trajectory to touchdown on the Martian surface.³

TPS Sizing Approach

To determine the required thickness of each layer for a given node on the vehicle, a three step sizing process was used for the dual layer system. First, only the entry portion of the trajectory was run with the insulator as the only protecting material ensuring that the RTV reaches exactly its allowable temperature (560 K). Next, keeping this thickness of the insulator, the entire aerocapsule and entry trajectory is simulated with an ablator on top of the insulator. In this case, the ablator is sized such that the maximum temperature of the insulator surface is equal to its maximum specified temperature (1700 K for LI-900). Finally, the whole trajectory is simulated again with the optimized thickness of the ablator now remaining constant while the insulator is resized until its thickness is again optimal for keeping the RTV maximum temperature at its threshold.

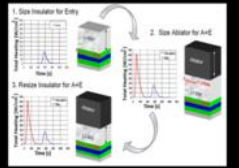


Fig. 3. Three step sizing process showing heat load experienced by the vehicle vs. time, the layer being sized in the material stack, and the constraining allowable temperature for each step.

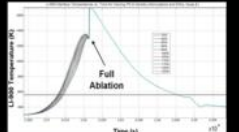


Fig. 4. Flow diagram depicting the computational tools and the flow of information in the sizing process.

Computational Approach

The ablation and thermal analysis tool used in the study was the Fully Implicit Ablation and Thermal Response Program (FIAT). In order to carry out the high volume of input file modifications, FIAT simulations, data organization, and post-processing, a custom MATLAB[®] architecture was constructed around FIAT.

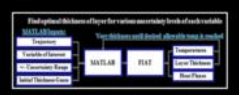


Fig. 5. LI-900 Surface Temperature vs. Time for the entry portion of the trajectory with varying PICA density. The temperature peak occurs after full ablation is constrained to 1700K to calculate optimal thickness of the ablator.

Results

The TPS sizing method was used to perform sensitivity analyses and performance characterization on a Mid LD vehicle at five different locations corresponding to five different values for the total integrated heat load seen throughout the aerocapsule + entry trajectory. This was done with both dual layer and traditional TPS.

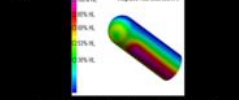


Fig. 6. The mid LD rigid aerobically vehicle with the five circled heat loads represent the heat loads investigated in this study.⁴

Key Parameters

An important milestone in this study was the identification of the variables to which the areal mass of the TPS was most sensitive. This sensitivity analysis was conducted on a node subject to 85% of the total heat load for both TPS constructions with PICA (Phenolic Impregnated Carbon Ablator) as the ablator in each case.

Heat Load	Material	Material	Material	Material	Material
85%	LI-900	LI-900	LI-900	LI-900	LI-900
85%	LI-900	LI-900	LI-900	LI-900	LI-900
85%	LI-900	LI-900	LI-900	LI-900	LI-900
85%	LI-900	LI-900	LI-900	LI-900	LI-900
85%	LI-900	LI-900	LI-900	LI-900	LI-900

Table 1. Summary of the areal mass variations due to +/- 3 sigma changes in system variables. The highlighted rows are the variables to which the system was most sensitive to.

Performance Sensitivities

After identifying the key sensitivities in the problem, the performance of both the dual layer and traditional TPS was compared directly using specific heat load, the parameter established in this study, as the metric of interest. Both the absolute performance and its sensitivity to changes in the variables previously identified were investigated. Below is a plot of specific heat load at the 85% node. The red and green lines are the nominal values for the dual and single layer constructions, respectively. The vertical bars indicate the range of variation in Q_{sp} due to +/- 3 sigma changes in each of the variables of interest.

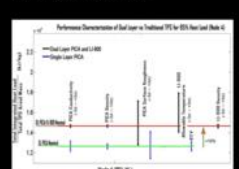


Fig. 7. Variations in Q_{sp} for variations in key parameters from their 3σ to -3σ uncertainty values. Note that surface roughness and allowable temperature reduce the greatest performance variation and the nominal performance of the dual layer is 16% greater than the traditional monolithic TPS.

Performance vs. Total Integrated Heat Load

When looking at results from only one reference node, as in Figure 7, one can see how changes in each variable impact the performance of the TPS. However, when this data is shown along with data from other heating conditions, conclusions about the relationship between heat load, overall performance, and sensitivity can be drawn. In Figure 8, this data is shown in the same form as in Figure 7, with the performance variations for due to each variable displayed. In Figure 9, the Root-Sum-Square of the all the sensitivities for each heating node is plotted to present a sense of overall variability in the system performance as a function of heat load.

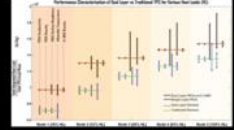


Fig. 8. Variations in Q_{sp} for variations in key parameters - all nodes. Note that sensitivities increase with heat load.

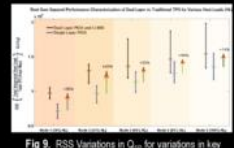


Fig. 9. RSS Variations in Q_{sp} for variations in key parameters - all nodes. Note that the relative benefit of the dual layer system is highest in the low heating environment.

Conclusions

A study was conducted with a new dual layer thermal protection system and the traditional single layer TPS to identify sensitivities in performance to uncertainties in material properties and aerothermal environments. A performance metric, Specific Heat Load, was developed in order to directly compare the results of the traditional, dual layer and eventually, flexible systems. Overall sensitivity in performance increased with increasing heat load for both systems as well as absolute performance. The relative benefit of the dual layer system over the traditional TPS is substantial across the board, but decreases as the heat load increases. At the lowest heat load investigated here, the relative improvement was 36% and at full heat load the benefit was 14%.

Literature cited

- 1) R.T. Edquist, et al. "Aerothermochemical Design of the Mars Science Laboratory Heatshield." AIAA Paper 2009-2075, AIAA Thermophysics Conference, San Antonio, Texas, June 2009.
- 2) J. Heemmen, et al. "Silica Impregnated Refractory Ceramic Ablator (SIRCA) for Jet Engine." November 2006.
- 3) Y.K. Chen & F.S. Milos. "Ablation and Thermal Response Program for Spacecraft Heatshield Analysis." Journal of Spacecraft and Rockets, Vol. 36, No. 3, 1999, pp. 472-482.
- 4) "Entry, Descent and Landing Systems Analysis Study. Phase 1 Report." NASA/TM-2005-216720.
- 5) M.S. McInnes. "Dual Heat Pulse, Dual Layer Thermal Protection System Sizing Analysis and Trade Studies for Human Mars Entry, Descent and Landing." AIAA-2011-143-660.
- 6) "World-Class Thermal Protection System (TPS) Margin Management Plan." NASA-ARC, CTPSA-A-DOC-7005, Rev. 2/0, Nov. 12, 2009.

PIGS IN SPACE: EFFECT OF ZERO GRAVITY AND AD LIBITUM FEEDING ON WEIGHT GAIN IN CAVIA PORCELLUS

Colin B. Purrington*
6673 College Avenue, Swarthmore, PA 19081 USA

ABSTRACT:

One ignored benefit of space travel is a potential elimination of obesity, a chronic problem for a growing majority in many parts of the world. In theory, when an individual is in a condition of zero gravity, weight is eliminated. Indeed, in space one could conceivably follow ad libitum feeding and never even gain an gram, and the only side effect would be the need to upgrade one's stretchy pants ("exercise pants"). But because many diet schemes start as very good theories only to be found to be rather harmful, we tested our predictions with a long-term experiment in a colony of Guinea pigs (*Cavia porcellus*) maintained on the International Space Station. Individuals were housed separately and given unlimited amounts of high-calorie food pellets. Fresh fruits and vegetables were not available in space so were not offered. Every 30 days, each Guinea pig was weighed. After 5 years, we found that individuals, on average, weighed nothing. In addition to weighing nothing, no weight appeared to be gained over the duration of the protocol. If space continues to be gravity-free, and we believe that assumption is sound, we believe that sending the overweight — and those at risk for overweight — to space would be a lasting cure.

INTRODUCTION:

The current obesity epidemic started in the early 1960s with the invention and proliferation of elastane and related stretchy fibers, which released wearers from the rigid constraints of clothes and permitted monthly weight gain without the need to buy new outfits. Indeed, exercise today for hundreds of million people involve only the act of wearing stretchy pants in public, presumably because the constrictive pressure forces fat molecules to adopt a more compact tertiary structure (Xavier 1965).

Luckily, at the same time that fabrics became stretchy, the race to the moon between the United States and Russia yielded a useful fact: gravity in outer space is minimal to nonexistent. When gravity is zero, objects cease to have weight. Indeed, early astronauts and cosmonauts had to secure themselves to their ships with seat belts and sticky boots. The potential application to weight loss was noted immediately, but at the time travel to space was prohibitively expensive and thus the issue was not seriously pursued. Now, however, multiple companies are developing cheap extra-orbital travel options for normal consumers, and potential travelers are also creating new ways to pay for products and services that they cannot actually afford. Together, these factors open the possibility that moving to space could cure overweight syndrome quickly and permanently for a large number of humans.

We studied this potential by following weight gain in Guinea pigs, known on Earth as fond of ad libitum feeding. Guinea pigs were long envisioned to be the "Guinea pigs" of space research, too, so they seemed like the obvious choice. Studies on humans are of course desirable, but we feel this current study will be critical in acquiring the attention of granting agencies.

MATERIALS AND METHODS:

One hundred male and one hundred female Guinea pigs (*Cavia porcellus*) were transported to the International Space Laboratory in 2010. Each pig was housed separately and deprived of exercise wheels and fresh fruits and vegetables for 48 months. Each month, pigs were individually weighed by duct-taping them to an electronic balance sensitive to 0.0001 grams. Back on Earth, an identical cohort was similarly maintained and weighed. Data was analyzed by statistics.

RESULTS:

Mean weight of pigs in space was 0.0000 +/- 0.0002 g. Some individuals weighed less than zero, some more, but these variations were due to reaction to the duct tape, we believe, which caused them to be alarmed and pushed against the force plate in the balance. Individuals on the Earth, the control cohort, gained about 240 g/month (p = 0.0002). Males and females gained a similar amount of weight on Earth (no main effect of sex), and size at any point during the study was related to starting size (which was used as a covariate in the ANCOVA). Both Earth and space pigs developed substantial dewlaps (double chins) and were lethargic at the conclusion of the study.

CONCLUSIONS:

Our view that weight and weight gain would be zero in space was confirmed. Although we have not replicated this experiment on larger animals or primates, we are confident that our result would be mirrored in other model organisms. We are currently in the process of obtaining necessary human trial permissions, and should have our planned experiment initiated within 60 years, pending expedited review by local and Federal IRBs.

ACKNOWLEDGEMENTS:

I am grateful for generous support from the National Research Foundation, Black Hole Diet Plans, and the High Fructose Sugar Association. Transport flights were funded by SPACE-EXES, the consortium of wives divorced from insanelly wealthy space-flight startups. I am also grateful for comments on early drafts by Mañana Athletic Club, Corpus Christi, USA. Finally, sincere thanks to the Cuy Foundation for generously donating animal care after the conclusion of the study.

LITERATURE CITED:

NASA. 1982. Project STS-XX: Guinea Pigs. Leaked internal memo.
Sekulic, S.R., D. D. Lukač, and N. M. Naumović. 2005. The Fetus Cannot Exercise Like An Astronaut: Gravity Loading Is Necessary For The Physiological Development During Second Half Of Pregnancy. Medical Hypotheses, 64:221-228.
Xavier, M. 1965. Elastane Purchases Accelerate Weight Gain in Case-control Study. Journal of Obesity, 2:23-40.

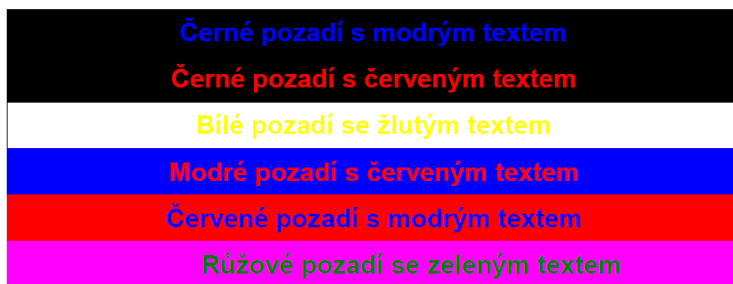
copyright colin purrington
<http://colinpurrington.com/tips/academic/posterdesign>



SPACE-EXES

BARVY

Nevhodné kombinace



Používat méně syté barvy, tak aby pozadí neodvádělo od textu
Používat spíše světlých, pastelových barev



Drug Distribution to Retinal Pigment Epithelium: Studies on Melanin Binding, Cellular Kinetics and SPECT/CT Imaging

Anna-Kaisa Rimpelä¹, M. Schmitt¹, S. Latonen¹, M. Hagström¹, M. Antopolsky¹, J. A. Manzanarez², H. Kidron¹, A. Urtti¹

¹Centre for Drug Research, Division of Pharmaceutical Biosciences, University of Helsinki, Finland

²Department of Thermodynamics, Faculty of Physics, University of Valencia, Spain

anna-kaisa.rimpela@helsinki.fi

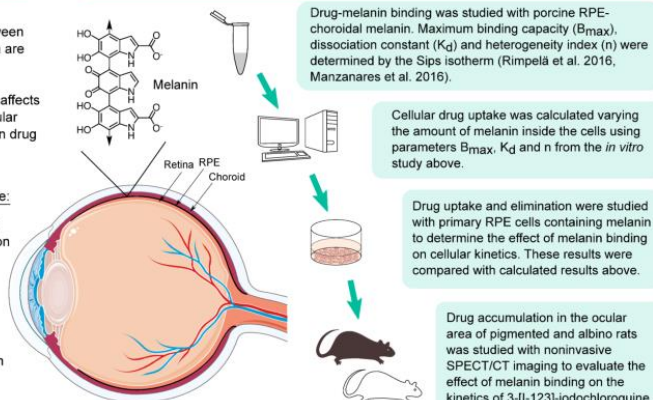
1 Purpose

Retinal pigment epithelium (RPE) is a densely pigmented cell monolayer between the neural retina and the choroid, which are drug targets for many diseases in the posterior part of the eye. The pigment, melanin, binds many clinical drugs and affects their pharmacokinetics and effect in ocular tissues. The effect of melanin binding on drug distribution to the RPE is inadequately understood.

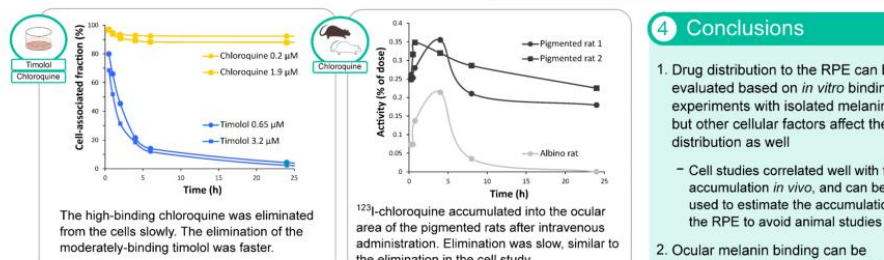
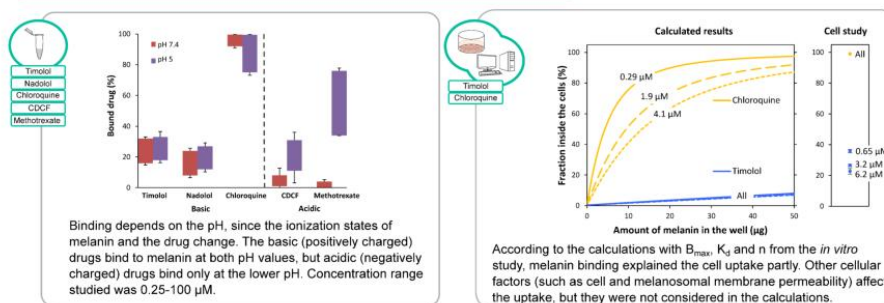
The aims of the study were to evaluate:

- If the extent of drug uptake to primary RPE cells could be estimated based on *in vitro* binding studies with isolated melanin and if cellular accumulation represents the accumulation *in vivo*.
- If single photon emission computed tomography/computed tomography (SPECT/CT) imaging could be used in studying pigment binding *in vivo* with pigmented and albino rats.

2 Methods



3 Results



4 Conclusions

- Drug distribution to the RPE can be evaluated based on *in vitro* binding experiments with isolated melanin, but other cellular factors affect the distribution as well
 - Cell studies correlated well with the accumulation *in vivo*, and can be used to estimate the accumulation to the RPE to avoid animal studies
- Ocular melanin binding can be monitored *in vivo* with non-invasive SPECT/CT imaging

References: Rimpelä et al. Mol Pharmaceutics 13(9): 2077-86, 2016. Manzanarez et al. Mol Pharmaceutics 13(4): 1251-7, 2016. Figure of the eye: modified from Servier Medical Art (<https://creativecommons.org/licenses/by/3.0/>)
Acknowledgements: Academy of Finland, University of Helsinki Doctoral Program in Drug Research, Orion Research Foundation

PROGRAMY

- CorelDraw
- Adobe Illustrator
- Latex
- PageMaker
- QUARK Express
- MS Power Point

PREZENTACE

Formou panelů – tisknuté postery

Formou zobrazení dataprojektorem – digitální prezentace

Formou webové aplikace – bez zpětné vazby